Wall Clutter Mitigation for Radar Imaging of Indoor Targets: A Matrix Completion Approach

Van Ha Tang
Faculty of Information Technology
Le Quy Don Technical University
236 Hoang Quoc Viet Street, Hanoi, Vietnam
Email: hatv@lqdtu.edu.vn

Abdesselam Bouzerdoum* and Son Lam Phung
School of Electrical, Computer and
Telecommunications Engineering,
University of Wollongong, Australia
*Also with the College of Science and Engineering,
Hamad Bin Khalifa University, Doha, Qatar
Email: a.bouzerdoum@uow.edu.au, phung@uow.edu.au

***Abstract*—This paper presents a low-rank matrix completion approach to tackle the problem of wall clutter mitigation for through-wall radar imaging in the compressive sensing context. In particular, the task of wall clutter removal is reformulated as a matrix completion problem in which a low-rank matrix containing wall clutter is reconstructed from compressive measurements. The proposed model regularizes the low-rank prior of the wall-clutter matrix via the nuclear norm, casting the wall-clutter mitigation task as a nuclear-norm penalized least squares problem. To solve this optimization problem, an iterative algorithm based on proximal gradient technique is introduced. Experiments on simulated full-wave electromagnetic data are conducted under compressive sensing scenarios. The results show that the proposed matrix completion approach is very effective at suppressing unwanted wall clutter and enhancing the desired targets.**

I. Introduction

In remote sensing operations, through-the-wall radar imaging (TWRI) has captured increasing research interests because of its abilities to sense through enclosed structures. The capability of imaging through walls is very useful for many civilian and military applications, such as search-and-rescue operations in a fire or earthquake disaster and hidden hostage localizations in a police mission [1]–[4]. However, unlike free-space radar imaging, in TWRI the strong front-wall electromagnetic (EM) returns dominate the backscattered radar targets and mask the targets in the formed image [5]–[8]. Thus, prior to image formation, mitigating the wall clutter is vital for target detection and identification.

Conventionally, through-wall radar (TWR) sensing techniques for stationary targets [9]–[12] assume having the data collected from an empty scene without targets. The empty-scene data is used to subtract wall clutter. This scheme is effective in mitigating wall interferences, but is unfeasible in practice. Therefore, several studies have been proposed for mitigating strong wall clutter without using the data collected from the reference scene [5]–[8]. In [5], a spatial filtering (SF) technique was introduced for wall-clutter suppression. This technique exploits the invariant characteristic of the wall returns and applies a notch filter to the antenna signals for removing low spatial frequencies containing constant wall contributions. In [6, 7], a subspace projection (SP) approach was proposed for segregating the target signals from the wall reverberations. This method considers the strength of the wall reflections over that of the target signals. It first computes singular value decomposition (SVD) based on the radar signal matrix to determine the wall-subspace, and then performs orthogonal SP to suppress the wall reflections from the received antenna signals. In [8], an adaptive Bayesian method was developed to learn the wall subspace from the received data. These approaches, however, are suitable only for full sensing operations; they require full data measurements for effective wall clutter reduction.

Recently, TWRI was investigated using compressive sensing (CS) framework [13]–[15] for accelerated data acquisition and relaxed system logistics. It has been shown in [16]–[18] that CS enables high-quality image formation even if data measurements are missing. Note that before applying CS, wall interferences need to be suppressed. However, because only reduced measurements are available, existing wall clutter reduction techniques are not effective if applied directly. To overcome this issue, wall clutter alleviation in the CS context typically consists of two stages [16]–[19]: (i) antenna signal estimation and (ii) wall clutter reduction. Prior to applying a wall clutter reduction technique, the antenna signal estimations have to be performed using incomplete measurements. In other words, these two-stage clutter mitigation approaches alleviate the effects of wall reflections by first estimating missing measurements and then including a wall-clutter mitigation technique. However, they may face the issue of multi-stage uncertainties because the signal estimation and wall clutter mitigation tasks are performed separately.

This paper proposes a low-rank matrix completion (LR-MC) approach for wall clutter removal in compressive TWR sensing context. The proposed approach formulates the problem of wall clutter mitigation as a regularized least squares (LS) optimization problem, whose objective function consists of a LS term, and a nuclear-norm penalty term. The LS term measures the error bound, and the nuclear-norm term is a relaxed regularization for the low-rank property introduced over the wall-clutter component. Given the matrix with missing measurements, the goal is to estimate a rank-deficiency matrix containing the wall reflections. To solve the optimization prob-

978-1-5386-0743-5/17/$31.00 ©2017 IEEE

lem, this paper introduces an iterative shrinkage algorithm, based on proximal gradient technique. The proposed algorithm is fast and suitable for large-sized problems, as the case of TWRI.

The paper is structured as follows. Section II presents the mathematical formulations in TWRI. Section III describes the proposed rank-deficiency matrix completion approach for wall clutter mitigation in compressive TWRI. Section IV describes the experimental results. Section V gives the concluding remarks.

II. Through-wall radar signal model

This section shortly describes the signal model of a monostatic stepped-frequency TWR system used to image targets situated in a behind-the-wall scene. The scene comprising P targets is sensed by moving a transceiver parallel to the wall, making an N-element synthetic aperture. Each antenna transceives a stepped-frequency signal having M frequencies equally divided among the bandwidth. The signal received by the n-th antenna for the m-th frequency, $z_{m,n}$, is modeled as

$$z_{m,n} = z^w_{m,n} + z^t_{m,n} + \upsilon_{m,n}, \tag{1}$$

where $z^w_{m,n}$ is the wall clutter, $z^t_{m,n}$ is the target return, and $\upsilon_{m,n}$ is the noise. The wall reflection $z^w_{m,n}$ is computed as

$$z^w_{m,n} = \sum_{r=1}^{R} \sigma_w a_r e^{-j2\pi f_m \tau^r_{n,w}}, \tag{2}$$

where R denotes the number of wall reverberations, σ_w is the wall reflectivity, a_r is the losing factor of the r-th wall path, and $\tau^r_{n,w}$ is the traveling delay of the r-th wall return. The target signal is considered as a superposition of all the target returns:

$$z^t_{m,n} = \sum_{p=1}^{P} \sigma_p e^{-j2\pi f_m \tau_{n,p}}, \tag{3}$$

where σ_p is the p-th target reflectivity, and $\tau_{n,p}$ is the signal traveling time from the n-th transceiver to the p-th target.

To form a target image, the scene is divided into a rectangular grid along the crossrange (horizontal) and downrange (vertical) with Q pixels. Let s_q denote a weighting identification function that represents the p-th target reflectivity:

$$s_q = \begin{cases} \sigma_p, & \text{if the } q\text{-th pixel includes the } p\text{-th target;} \\ 0, & \text{otherwise.} \end{cases} \tag{4}$$

Supposing the target comprising points situated on the pixels, from (3) we have a matrix-vector form representing the target return at the n-th antenna:

$$\mathbf{z}^t_n = \mathbf{\Psi}_n \, \mathbf{s}, \tag{5}$$

where $\mathbf{z}^t_n = [z^t_{1,n}, \ldots, z^t_{M,n}]^T$, $\mathbf{s} = [s_1, \ldots, s_Q]^T$, $\mathbf{\Psi}_n$ being an $M \times Q$ matrix with $\psi_n(m,q) = \exp(-j2\pi f_m \tau_{n,q})$, and $\tau_{n,q}$ denoting the focusing delay. Stacking all measurements collected from the N antennas yields

$$\mathbf{z}^t = \mathbf{\Psi} \, \mathbf{s}, \tag{6}$$

where $\mathbf{z}^t = [(\mathbf{z}^t_1)^T, \ldots, (\mathbf{z}^t_N)^T]^T$, and $\mathbf{\Psi} = [\mathbf{\Psi}^T_1, \ldots, \mathbf{\Psi}^T_N]^T$.

From (6), the target image $\mathbf{s}$ can be recovered from the target signal $\mathbf{z}^t$ using CS technique or delay-and-sum (DS) beamforming. The CS aims to promote sparsity of the image $\mathbf{s}$; the image is obtained by solving an ℓ_1-regularization problem. The DS beamforming method is only effective if full measurements are available. Note that in practice the target signal $\mathbf{z}^t$ is unavailable. Instead, we have only the radar signal $\mathbf{z}$, which is the target signal corrupted by the wall component $\mathbf{z}^w$ and noise $\boldsymbol{\upsilon}$. Thus, prior to image formation, the target component needs to be segregated from the wall interferences. Wall-clutter rejection methods, such as SF [5] or SP [7], can be applied if the same frequency measurements are available at all antennas. In general compressive sensing TWR, however, only a subset of frequency samples is acquired, which may vary from one spatial position to another. To address this issue, two-stage wall clutter mitigation techniques have been proposed, where the missing measurements are first estimated, followed by wall-clutter suppression applied to the estimated measurements. The issue with the two-stage approaches is that the performance relies on the signal recovery accuracy. In this paper, the wall-clutter removal task is formulated as a low-rank matrix completion problem, which is described in the following sections.

III. Low-rank matrix completion TWRI

This section presents a LR-MC approach for clutter removal in compressive TWRI. First, the measurements received from the antenna positions are represented in matrix-form. Then, the problem of estimating the wall contributions is cast as a regularized least squares minimization problem, in which the nuclear-norm penalty is enforced for the low-rank structure of the wall-clutter matrix. In Subsection III-A, the formulation of the regularized least squares optimization problem is described. In Subsection III-B, an iterative algorithm is developed for solving the minimization problem.

A. Formulation of matrix completion problem

The radar signals received at all N antennas for M frequencies can be represented in matrix-form. From (1), we have

$$\mathbf{Z} = \mathbf{Z}^w + \mathbf{Z}^t + \mathbf{\Upsilon}, \tag{7}$$

where $\mathbf{Z} = [z_{m,n}]$, $\mathbf{Z}^w = [z^w_{m,n}]$, $\mathbf{Z}^t = [z^t_{m,n}]$, and $\mathbf{\Upsilon} = [\upsilon_{m,n}]$ are $M \times N$ matrices representing, respectively, the antenna signals, the wall clutter, the target signals, and the noise.

In compressive sensing TWRI scenario, we assume that a reduced subset of K measurements ($K \ll M \times N$) is collected. Let $\mathbf{\Phi} \in \mathbb{R}^{K \times MN}$ be a selection matrix. This matrix has only one unitary element in each row used to select one frequency for one antenna location. The compressed measurement vector $\mathbf{y} \in \mathbb{C}^K$ is mathematically expressed as

$$\mathbf{y} = \mathbf{\Phi} \, \mathrm{vec}(\mathbf{Z}) = \mathcal{A}(\mathbf{Z}). \tag{8}$$

Here, $\mathrm{vec}(\mathbf{Z})$ is the vectorization operator arranging the columns of $\mathbf{Z}$ into a composite column vector. Note that $\mathbf{Z}$

can be obtained from $\mathbf{y}$ as $\mathbf{Z} = \mathrm{mat}(\mathbf{\Phi}^\dagger\, \mathbf{y}) = \mathcal{A}^*(\mathbf{y})$, where mat represents the operator forming a vector of size $MN \times 1$ into an $M \times N$ matrix, and † is the pseudo-inverse operator.

Given the compressed measurement vector $\mathbf{y}$, our aim is to estimate the wall matrix $\mathbf{Z}^w$, exploiting the low-rank representation of $\mathbf{Z}^w$. The justification is that in TWR sensing, the wall signals lie in a low-dimensional subspace [7, 20]. The task of estimating the rank-deficiency matrix $\mathbf{Z}^w$ is achieved via solving the following matrix completion problem [21]–[23]:

$$\min_{Z^w} \quad \|\mathbf{Z}^w\|_* \quad \text{subject to} \quad \|\mathbf{y} - \mathcal{A}(\mathbf{Z}^w)\|_2^2 \leq \epsilon. \tag{9}$$

In (9), $\|\mathbf{Z}^w\|_*$ denotes the nuclear-norm (the sum of the singular values of $\mathbf{Z}^w$), and ϵ measures a noise bound. The nuclear-norm penalty is the convex relaxation of rank minimization. To solve Problem (9) efficiently, we cast it into an unconstrained version or its Lagrangian form:

$$\min_{Z^w} \;\; f(\mathbf{Z}^w) = \frac{1}{2}\,\|\mathbf{y} - \mathcal{A}(\mathbf{Z}^w)\|_2^2 + \gamma\,\|\mathbf{Z}^w\|_*\,, \tag{10}$$

where γ is a positive parameter. Convex analysis can be used to show the equivalence between of the solutions of (9) and (10). In the next subsection, we introduce an iterative algorithm that can estimate the wall clutter $\mathbf{Z}^w$ by minimizing $f(\mathbf{Z}^w)$.

B. Iterative algorithm

This subsection presents an iterative algorithm to solve Problem (10). First, let us consider the more general case of minimizing a composite objective function:

$$\min_{\mathbf{x}} f(\mathbf{x}) = g(\mathbf{x}) + \gamma\, h(\mathbf{x}), \tag{11}$$

where $g(\mathbf{x})$ is differentiable, convex, and smooth (the quadratic term in (10)) and $h(\mathbf{x})$ is convex but not necessary smooth (the nuclear norm in (10)). This problem is solved efficiently using *proximal gradient technique*. Let $\mathbf{x}_i$ be an estimate of the solution at the i-th iteration. Then, the next estimate of the minimizer is obtained by solving:

$$\mathbf{x}_{i+1} = \arg\min_{\mathbf{x}} \frac{1}{2}\,\|\mathbf{u}_i - \mathbf{x}\|_2^2 + \gamma\alpha\, h(\mathbf{x}), \tag{12}$$

where $\mathbf{u}_i = \mathbf{x}_i - \alpha\nabla g(\mathbf{x}_i)$. Here, $\nabla g(\mathbf{x}_i)$ denotes the gradient of $g(\mathbf{x})$ evaluated at the current estimate $\mathbf{x}_i$. When ∇g is a Lipschitz continuous function with constant C, this method converges if $\alpha \in (0,\ 1/C]$. This generic optimization technique and its convergence guarantees have been widely used to solve the minimization problem (11) under different names: proximal gradient method [24], thresholded Landweber iteration [25], iterative shrinkage/thresholding [26], or separable approximation [27].

Here we use the iterative technique in (12) to solve the problem in (10). Following this strategy, minimizing $f(\mathbf{Z}^w)$ produces a sequence of estimates $\{\mathbf{Z}_i^w\}$. Using the technique in (12), Problem (10) can be minimized iteratively:

$$\mathbf{Z}_{i+1}^w = \arg\min_{\mathbf{Z}^w} \frac{1}{2}\|\mathbf{Z}_i - \mathbf{Z}^w\|_F^2 \;+\; \gamma\alpha\|\mathbf{Z}^w\|_*, \tag{13}$$

where $\|\cdot\|_F$ is the Frobenius norm, and the auxiliary variable $\mathbf{Z}_i$ plays the role of $\mathbf{u}_i$ in (12),

$$\mathbf{Z}_i = \mathbf{Z}_i^w - \alpha\,\mathcal{A}^*(\mathcal{A}(\mathbf{Z}_i^w) - \mathbf{y}). \tag{14}$$

To ensure convergence of $\{\mathbf{Z}_i^w\}$ to a minimizer of (10), α is required to satisfy $\alpha \in (0, 1/\|\mathbf{\Phi}\|_2^2]$. Hereafter, $\|\mathbf{\Phi}\|_2$ represents the spectral-norm of $\mathbf{\Phi}$, being the maximum singular value of the matrix.

The task now is to solve the relaxed rank-minimization problem (13). Using the *singular value thresholding* (SVT) technique, a closed-form solution to (13) is obtained by the following theorem [28, 29]:

Theorem 1: For $\tau \geq 0$ and $\mathbf{Z} \in \mathbb{C}^{M\times N}$, the singular value soft-thresholding $\mathcal{S}_\tau(\mathbf{Z})$ obeys

$$\mathcal{S}_\tau(\mathbf{Z}) = \arg\min_{\mathbf{Z}^w} \frac{1}{2}\,\|\mathbf{Z} - \mathbf{Z}^w\|_F^2 + \tau\,\|\mathbf{Z}^w\|_*\,. \tag{15}$$

Theorem 1 can be proved based on the concept of proximal gradient of convex functions (here the nuclear-norm). Let us consider the standard soft-thresholding:

$$\mathcal{T}_\tau(x) = \mathrm{sign}(x)\max(|x|-\tau, 0) = \frac{x}{|x|}\max(|x|-\tau, 0). \tag{16}$$

The SVT operator in (15) is computed as

$$\mathcal{S}_\tau(\mathbf{Z}) = \mathbf{U}\,\mathcal{T}_\tau(\mathbf{\Lambda})\,\mathbf{V}^H, \tag{17}$$

where $\mathbf{Z} = \mathbf{U}\,\mathbf{\Lambda}\,\mathbf{V}^H$ is the SVD of $\mathbf{Z}$. Note that when applied to vectors or matrices, the soft-thresholding operator $\mathcal{T}_\tau(\cdot)$ performs entrywise. Using Theorem 1, the solution to Problem (13) is given by

$$\mathbf{Z}_{i+1}^w = \mathcal{S}_{\gamma\alpha}(\mathbf{Z}_i). \tag{18}$$

In summary, the iterative steps for solving Problem (10) are provided in Table I, which is referred as Algorithm 1. This algorithm takes an input set of the data matrix $\mathbf{y}$, the parameters α, γ, and a predefined tolerance tol. The parameter α is regarded as a gradient step-size and set to the largest possible value for accelerated convergence, whereas the regularization parameter γ is problem-dependent and needs to be tuned appropriately. In the processing steps, this algorithm performs a gradient evaluation (Step 2) and uses the resultant matrix as input for wall clutter estimation (Step 3) via SVT technique. The algorithm stops when it converges to a local optimum. In implementation, the algorithm terminates when the relative change of the objective function becomes negligible (Step 4).

For image formation, the estimated wall clutter matrix is subtracted from the compressed measurements to obtain the clutter-free data. Let $\hat{\mathbf{Z}}^w$ denote the estimated wall clutter matrix as the output of Algorithm 1. From (6), (7), and (8), we can formulate a linear model relating the target measurement vector $\mathbf{y}^t$ to the target image $\mathbf{s}$:

$$\mathbf{y}^t = \mathbf{y} - \mathbf{\Phi}\,\mathrm{vec}(\hat{\mathbf{Z}}^w) = \mathbf{\Phi}\mathbf{\Psi}\,\mathbf{s} + \boldsymbol{\upsilon}, \tag{19}$$

TABLE I
ALGORITHM 1: PROXIMAL GRADIENT ITERATIVE ESTIMATIONS OF WALL CLUTTER IN COMPRESSIVE TWRI.

1) Initialization: Set $\mathbf{Z}_0^w \leftarrow \mathcal{A}^*(\mathbf{y})$, and $i \leftarrow 0$.

2) Perform gradient splitting using (14):

$\mathbf{Z}_i \leftarrow \mathbf{Z}_i^w - \alpha\mathcal{A}^*(\mathcal{A}(\mathbf{Z}_i^w) - \mathbf{y})$.

3) Estimate wall component using (18):

$\mathbf{Z}_{i+1}^w \leftarrow \mathcal{S}_{\alpha\gamma}(\mathbf{Z}_i)$.

4) Compute the cost function $f(\mathbf{Z}_{i+1}^w)$ using (10) and

if $\frac{|f(\mathbf{Z}_{i+1}^w) - f(\mathbf{Z}_i^w)|}{|f(\mathbf{Z}_i^w)|} < \text{tol}$ then terminate the algorithm,

otherwise increment $i \leftarrow i + 1$ and go to Step 2.

where we have defined $\text{vec}(\mathbf{Z}^t) = \mathbf{\Psi}\,\mathbf{s}$ and $\mathbf{\Phi}\,\text{vec}(\mathbf{\Upsilon}) = \boldsymbol{\upsilon}$. Now a sparse image of the indoor target $\mathbf{s}$ is obtained by solving the following ℓ_1 minimization:

$$\mathbf{s} = \arg\min_{\mathbf{s}} \frac{1}{2}\|\mathbf{y}^t - \mathbf{\Phi}\mathbf{\Psi}\mathbf{s}\|_2^2 + \lambda\|\mathbf{s}\|_1. \tag{20}$$

Note that Problem (20) is solved efficiently using the proximal gradient technique described in (11) and (12). Here, we apply the soft-thresholding operator (16) to the auxiliary variable obtained in a similar manner to (14).

IV. EXPERIMENTAL RESULTS

This section describes experimental results obtained using electromagnetic data. The datasets were acquired using the XFdtd software[1] via the simulations with Finite Difference Time Domain technique.

A. Experimental method

Data acquisition was conducted using a synthetic aperture radar system with stepped-frequency principles. A linear antenna array was synthesized by moving the transceiver parallel to a concrete wall with 0.15 m thickness, at a standoff distance of 1 m. The antenna array has 51 elements, with inter-element distance of 0.024 m. The scene is imaged by transceiving a stepped-frequency signal of 1 GHz bandwidth, having 334 steps with step-size being 3 MHz. Fig. 1 shows the scene layout containing the front wall and two dihedral targets.

The proposed algorithm requires a set of input parameters, which were chosen as follows. The gradient step-size α is set to $\alpha = 1/\|\mathbf{\Phi}\|_2^2$ for accelerated convergence. The regularization parameter γ is selected as $\gamma = 10^{-2}\|\mathcal{A}^*(\mathbf{Y})\|_2$. The algorithm is deemed to have converged if the relative change of the objective function is smaller than $\text{tol} = 10^{-4}$ (see Step 4 in Algorithm 1).

The performance of different TWRI techniques is measured using the target-to-clutter ratio (TCR) (in dB). Let A_t and A_c, respectively, be the target and clutter regions of the formed image I. Denote N_t and N_c, respectively, be the number of target and clutter pixels. The TCR is defined as

$$\text{TCR} = 10\log_{10}\left(\frac{\frac{1}{N_t}\sum_{q\in A_t}|I_q|^2}{\frac{1}{N_c}\sum_{q\in A_c}|I_q|^2}\right). \tag{21}$$

Note that the clutter region is considered as the whole image excluding the target region.

[1]Website: www.remcom.com

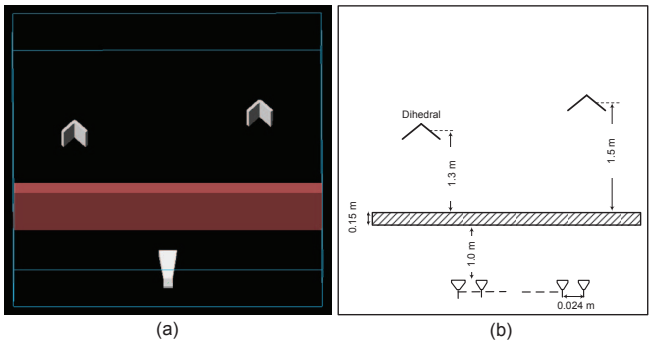

Fig. 1. Through-wall radar data collection: (a) geometric scene design, (b) top-view of the indoor scene.

B. Comparison with two-stage signal estimation & wall clutter mitigation

In the first experiment, a reduced dataset accounting for only 50% of the full measurements is used for clutter suppression and image formation. The dataset was generated by randomly selecting only 167 (50%) of total frequencies at all antenna locations and hence the frequency measurements differ across antennas. For comparison, two-stage approaches, signal estimation followed by wall-clutter mitigation, are implemented on the same dataset. In these two-stage approaches, the missing measurements are first recovered, followed by a SF [5] or a SP technique [7] for wall-clutter mitigation. The target image is formed by solving the ℓ_1 minimization problem (20).

Fig. 2 shows the images formed after different clutter mitigation methods. Without clutter removal, strong wall reverberations obscure the targets, making target identification very difficult, as illustrated in Fig. 2(a). Figs. 2(b) and (c) present the images reconstructed after using the two-stage signal estimation followed by spatial filtering and subspace projection for clutter reduction, respectively. Although the wall clutter mitigation techniques remove the strong wall reflections, the formed images still contain clutter residuals. By contrast, Fig. 2(d) illustrates the image formed after the proposed LR-MC method. It can be observed that the targets are well localized and the clutter is significantly suppressed.

To quantify the performances of the different clutter mitigation methods, the performance measure TCR is computed. Table II lists the TCRs of the images depicted in Fig. 2. It can be seen that the LR-MC approach yields the highest TCR value (30.67 dB) among the tested clutter mitigation techniques.

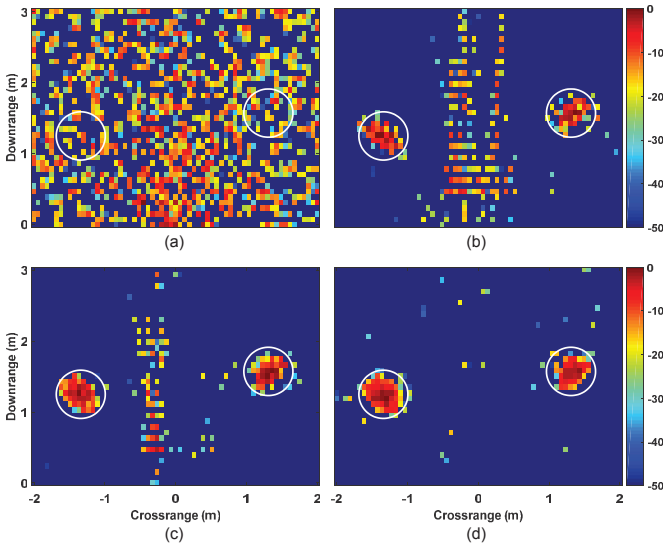

Fig. 2. Images reconstructed after applying different wall-clutter mitigation techniques using 50% of the total measurements: (a) without clutter mitigation, (b) two-stage signal estimation & spatial filtering, (c) two-stage signal estimation & subspace projection, and (d) proposed LR-MC approach.

TABLE II
TCR OF THE IMAGES RECONSTRUCTED AFTER APPLYING DIFFERENT CLUTTER MITIGATION APPROACHES USING 50% DATA MEASUREMENTS.

Wall clutter mitigation method	**TCR (dB)**
Proposed low-rank matrix completion method	**30.67**
Two-stage signal estimation & spatial filtering	17.68
Two-stage signal estimation & subspace projection	20.40
Without clutter mitigation	-2.39

C. Performance analysis of the proposed LR-MC algorithm

This subsection gives further insights into the proposed LR-MC iterative algorithm. This algorithm takes an input measurement set $\mathbf{y}$ and outputs the wall component matrix $\mathbf{Z}^w$ by minimizing the objective function $f(\mathbf{Z}^w)$, see (10). Iterative minimization produces a sequence of estimates $\{\mathbf{Z}_i^w\}$, starting from $\mathbf{Z}_0^w \leftarrow \mathcal{A}^*(\mathbf{y})$ and terminating when a local minimum is achieved. Note that this local minimum is also the global minimum because the objective function $f(\mathbf{Z}^w)$ is convex. The goal of optimization is to obtain a low-rank representation of the wall-clutter matrix $\mathbf{Z}^w$ using nuclear-norm penalty. Hence, during the minimization, the rank of $\mathbf{Z}^w$ should start from the largest possible value $(\min(M, N))$, decreases during the iteration, and converges to a low-rank representation of the wall contributions.

Fig. 3 demonstrates the rank values of $\mathbf{Z}^w$ recorded at different iterations to obtain the target image presented in Subsection IV-B. It is observed that the algorithm achieves a rank minimization of the wall-clutter matrix $\mathbf{Z}^w$. The rank of $\mathbf{Z}^w$ starts at 51 $(\min(334, 51))$, decreases during the loop, and reaches 1 at convergence. Likewise, Fig. 4 illustrates the convergence of the cost function $f(\mathbf{Z}^w)$. The value of the objective function is 277.31 at initialization, and it reduces during the loop, reaching 70.13 at convergence. Note that in the implementation, the algorithm stops if the relative change of the objective function is negligible. It can be observed from Fig. 4 that the changes of the objective function are negligible after the 36-th iteration. At the final iteration, the relative change of the objective function is 7.9×10^{-5}.

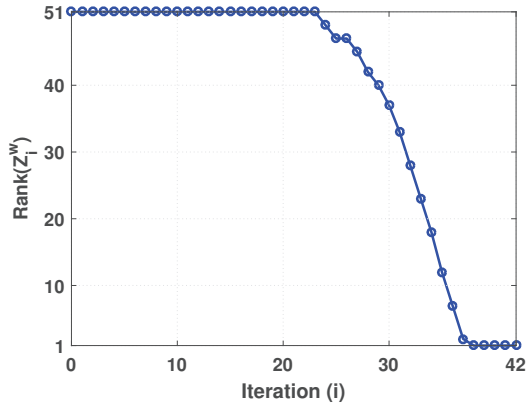

Fig. 3. The rank values of the estimated wall component $\mathbf{Z}^w$ during the loop: the rank decreasing from 51 at initialization to 1 at convergence. This result is recorded during the minimization using the 50% measurement set.

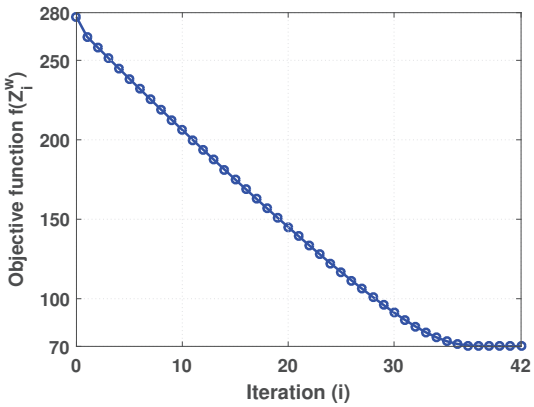

Fig. 4. The change of objective function $f(\mathbf{Z}^w)$ during minimization: the value starts at 277.31, decreases during the loop, and converges to a local minimum at 70.13. The relative change of the cost function at the 42-th iteration is 7.9×10^{-5}.

V. CONCLUSION

This paper presented a low-rank matrix completion approach for removing wall clutter in compressive through-the-wall radar imaging. The task of wall-clutter mitigation is formulated as a nuclear-norm regularized least squares minimization problem. An iterative algorithm based on proximal gradient technique is developed to solve the minimization problem, capturing the wall reflections. Experimental results using simulated EM radar data have confirmed the effectiveness of the proposed approach. It mitigates the wall reflections even if the measurements are missing. The proposed LR-MC model is more robust than the existing two-stage wall clutter mitigation methods in CS context; the LR-MC model estimates the wall clutter more precisely and enhances the quality of indoor image reconstruction.

ACKNOWLEDGMENTS

The work of V. H. Tang was supported by the Research Fund RFIT@LQDTU, Faculty of Information Technology, Le Quy Don Technical University. The work of A. Bouzerdoum and S. L. Phung was supported by a grant from the Australian Research Council (ARC).

REFERENCES

[1] M. G. Amin (Ed.), *Through-The-Wall Radar Imaging*. Boca Raton, FL: CRC Press, 2010.

[2] F. Ahmad *et al*., "Autofocusing of through-the-wall radar imagery under unknown wall characteristics," *IEEE Trans. Image Process.*, vol. 16, no. 7, pp. 1785–1795, Jul. 2007.

[3] V. H. Tang *et al*., "Two-stage through-the-wall radar image formation using compressive sensing," *Journal of Elect. Imaging*, vol. 22, no. 2, pp. 021 006.1–021 006.10, Apr.–Jun. 2013.

[4] C. H. Seng *et al*., "Probabilistic fuzzy image fusion approach for radar through wall sensing," *IEEE Trans. Image Process.*, vol. 22, no. 12, pp. 4938–4951, Dec. 2013.

[5] Y.-S. Yoon and M. G. Amin, "Spatial filtering for wall-clutter mitigation in through-the-wall radar imaging," *IEEE Trans. Geo. and Rem. Sen.*, vol. 47, no. 9, pp. 3192–3208, Sep. 2009.

[6] F. H. C. Tivive *et al*., "An SVD-based approach for mitigating wall reflections in through-the-wall radar imaging," *Proc. IEEE Radar Con.*, pp. 519–524, Kansas City, MO, May 2011.

[7] F. H. C. Tivive *et al*., "A subspace projection approach for wall clutter mitigation in through-the-wall radar imaging," *IEEE Trans. Geo. and Rem. Sen.*, vol. 53, no. 4, pp. 2108–2122, Apr. 2015.

[8] V. H. Tang *et al*., "A sparse Bayesian learning approach for through-wall radar imaging of stationary targets," *IEEE Trans. Aero. and Elec. Sys.*, Apr. 2017, online available: http://ieeexplore.ieee.org/document/7921613/.

[9] Y.-S. Yoon and M. G. Amin, "Compressed sensing technique for high-resolution radar imaging," in *Proc. SPIE: Sig. Proc., Sen. Fusion, and Target Rec. XVII*, Orlando, FL, Mar. 2008, pp. 69 681A.1– 69 681A.10.

[10] Q. Huang *et al*., "UWB through-wall imaging based on compressive sensing," *IEEE Trans. Geo. and Rem. Sen.*, vol. 48, no. 3, pp. 1408–1415, Mar. 2010.

[11] V. H. Tang *et al*., "Enhanced through-the-wall radar imaging using Bayesian compressive sensing," in *Proc. SPIE Comp. Sen. II*, vol. 8717, May 2013, pp. 87 170I.1–87 170I.12.

[12] J. Yang *et al*., "Multiple-measurement vector model and its application to through-the-wall radar imaging," *Proc. IEEE ICASSP*, pp. 2672–2675, Prague, Czech Republic, May 2011.

[13] D. L. Donoho, "Compressed sensing," *IEEE Trans. Inf. Theory*, vol. 52, no. 4, pp. 1289–1306, Apr. 2006.

[14] E. J. Candes *et al*., "Stable signal recovery from incomplete and inaccurate measurements," *Com. on Pure and Applied Math.*, vol. 59, no. 8, pp. 1207–1223, Aug. 2006.

[15] E. J. Candes and M. B. Wakin, "An introduction to compressive sampling," *IEEE Sig. Proc. Mag.*, vol. 25, no. 2, pp. 21–30, Mar. 2008.

[16] E. Lagunas *et al*., "Joint wall mitigation and compressive sensing for indoor image reconstruction," *IEEE Trans. Geo. and Rem. Sen.*, vol. 51, no. 2, pp. 891 – 906, Feb. 2013.

[17] V. H. Tang *et al*., "Enhanced wall clutter mitigation for through-the-wall radar imaging using joint Bayesian sparse signal recovery," *Proc. IEEE ICASSP*, pp. 7804–7808, Florence, Italy, May 2014.

[18] F. Ahmad *et al*., "Wall clutter mitigation using discrete prolate spheroidal sequences for sparse reconstruction of indoor stationary scenes," *IEEE Trans. Geo. and Rem. Sen.*, vol. 53, no. 3, pp. 1549–1557, Mar. 2015.

[19] F. H. C. Tivive *et al*., "Multi-stage compressed sensing and wall clutter mitigation for through-the-wall radar image formation," in *IEEE Sen. Array and Multi. Signal Process. Workshop*, A Coruna Spain, Jun. 2014, pp. 489–492.

[20] V. H. Tang *et al*., "Radar imaging of stationary indoor targets using joint low-rank and sparsity constraints," in *IEEE ICASSP*, Shanghai China, Mar. 2016, pp. 1412–1416.

[21] E. J. Candes and B. Recht, "Exact matrix completion via convex optimization," *Found. of Comp. Math.*, vol. 9, no. 6, pp. 717–772, Dec. 2009.

[22] E. J. Candes and Y. Plan, "Matrix completion with noise," *Proc. of the IEEE*, vol. 98, no. 6, pp. 925–936, Jun. 2010.

[23] R. Keshavan *et al*., "Matrix completion from noisy entries," in *NIPS Proc.*. Curran Asso., Inc., 2009, pp. 952–960.

[24] P. L. Combettes and V. R. Wajs, "Signal recovery by proximal forward-backward splitting," *SIAM Journal of Multi. Model. Sim.*, vol. 4, no. 4, pp. 1168–1200, Nov. 2006.

[25] C. Vonesch and M. Unser, "A fast thresholded Landweber algorithm for wavelet-regularized multidimensional deconvolution," *IEEE Trans. Image Process.*, vol. 17, no. 4, pp. 539–549, Apr. 2008.

[26] A. Beck and M. Teboulle, "A fast iterative shrinkage-thresholding algorithm for linear inverse problems," *SIAM Journal on Imaging Sci.*, vol. 2, no. 1, pp. 183–202, Mar. 2009.

[27] S. J. Wright *et al*., "Sparse reconstruction by separable approximation," *IEEE Trans. Signal Proc.*, vol. 57, no. 7, pp. 2479–2493, Jul. 2009.

[28] S. Ma *et al*., "Fixed point and Bregman iterative methods for matrix rank minimization," *Math. Prog.*, vol. 128, no. 1, pp. 321–353, Jun. 2011.

[29] J.-F. Cai *et al*., "A singular value thresholding algorithm for matrix completion," *SIAM Journal on Opti.*, vol. 20, no. 4, pp. 1956–1982, Mar. 2010.